InFRA: Interference-Aware PHY/FEC Rate Adaptation for Video Multicast over WLAN

Yeonchul Shin†, Gyujin Lee†, Junyoung Choi†, Jonghoe Koo†, Sung-Ju Lee‡, and Sunghyun Choi†
†Department of ECE and INMC, Seoul National University, Seoul, Korea
‡School of Computing, KAIST, Deajeon, Korea
Email: {ycshin, gjlee, jychoi, jhkoo}@mwnl.snu.ac.kr, profsj@kaist.ac.kr, schoi@snu.ac.kr

***Abstract*—Multi-rate forward erasure correction (FEC)-applied wireless multicast enables reliable and efficient video multicast with intelligent selection of physical (PHY) layer data rate and FEC rate. The optimal PHY/FEC rates depend on the cause of the packet losses. However, previous approaches select the PHY/FEC rates by considering only channel errors even when interference is also a major source of packet losses. We propose InFRA, an interference-aware PHY/FEC rate adaptation framework that (i) infers the cause of the packet losses based on received signal strength indicator (RSSI) and cyclic redundancy check (CRC) error notifications, and (ii) determines the PHY/FEC rates based on the cause of packet losses. Our prototype implementation with off-the-shelf chipsets demonstrates that InFRA enhances the multicast delivery under various network scenarios. InFRA enables 2.3x and 1.8x more nodes to achieve a target video packet loss rate with a contention interferer and a hidden interferer, respectively, compared with the state-of-the-art PHY/FEC rate adaptation scheme. To our best knowledge, InFRA is the first work to take the impact of interference into account for the PHY/FEC rate adaptation.**

I. Introduction

With the prevalence of mobile devices such as smartphones and tablets as well as the increase of capacity, the traffic volume of multimedia applications over the IEEE 802.11 wireless local area network (WLAN) has grown explosively during the last decade [1]. As one of the promising solutions for the explosion of multimedia traffic, multicast has attracted the interest from both the research community and industry practitioners, especially when sharing a common venue-specific video to multiple receivers, e.g., live video seminars and lectures in companies and live broadcast in sports stadiums and concert halls. Multicast services, however, have not been widely deployed as multicast over WLAN has inherent low reliability due to the absence of retransmission.[1]

Employing packet-level forward erasure correction (FEC) on multicast is a well-known reliability enhancement method. Each video frame is packetized, and a batch of the packets generate additional parity packets via FEC encoding, thus allowing each receiver to recover lost packets with the parity packets. The FEC rate, i.e., the ratio of the number of original packets (batch size, K) over the total number of original and parity packets (generation size, N), is a key design parameter.

Another challenge of video multicast is low efficiency as the physical (PHY) layer data rate for multicast is typically set to the lowest rate to serve even the user with the worst channel condition. Although multicast PHY rate adaptation allows access point (AP) to use a higher PHY rate depending on the situation, adapting only PHY rate is unreliable due to the lack of the loss recovery mechanism [3]. We believe that applying FEC with multicast PHY rate adaptation can realize reliable and efficient multicast service, with appropriate selection of PHY and FEC rates.

Although lowering either the PHY or FEC rate can reduce the packet losses, the impact could be different depending on the cause of packet losses. Decreasing the PHY rate lowers the required signal-to-interference plus noise ratio (SINR), thus allowing packets to be transmitted successfully even when the channel quality is poor. However, if a packet loss is caused by interference (e.g., collision), decreasing the PHY rate is not helpful [4]. On the other hand, decreasing the FEC rate, i.e., increasing N, enhances reliability, when interference is the dominant factor of packet losses, by increasing the opportunities of accessing the channel without interference. Lowering the FEC rate can be less effective than lowering the PHY rate when many packets are lost due to poor channel quality [5, 6]. Therefore, diagnosing the cause of packet losses enables us to select proper PHY/FEC rates.

We propose InFRA, an interference-aware PHY/FEC rate adaptation framework for the multi-rate FEC-applied wireless multicast system. In InFRA, each station (STA) periodically requests desired PHY/FEC rates, and the AP chooses the best PHY/FEC rates based on the requests from multiple STAs. InFRA diagnoses the cause of packet losses using received signal strength indicator (RSSI) and cyclic redundancy check (CRC) error notifications, which are both available in the standard. If a packet is lost, we infer it as due to the poor channel quality when an average RSSI of the associated batch is lower than a PHY rate-dependent threshold. Otherwise, we infer it as due to interference. We further classify the losses from interference depending on whether the CRC error notification exists.

Based on that, InFRA determines appropriate PHY/FEC rates to minimize the airtime consumption while meeting various performance requirements, e.g., the fraction of nodes satisfying the target application-layer packet loss rate (APLR).[2]

[1]IEEE 802.11aa [2] defines new retransmission protocols for multicast to improve reliability, yet they are not widely-adopted in off-the-shelf chipsets.

[2]We distinguish application-layer PLR, i.e., the PLR after FEC decoding, from the MAC-layer PLR (MPLR), i.e., the PLR before FEC decoding. For brevity, the packet loss and PLR indicate the MAC-layer packet loss and MPLR, respectively, unless noted otherwise.

When packet losses occur due to poor channel quality, InFRA decreases PHY rate while when packet losses happen due to interference, InFRA determines whether to decrease PHY rate or FEC rate based on the interfering signal strength and the number of packet losses.

Our key contributions are summarized as follows:

- We investigate the impact of interference on multi-rate FEC-applied multicast, and empirically verify the importance of interference-aware PHY/FEC rate selection.
- We propose a standard-compliant loss differentiation for multicast based on RSSI and CRC error notifications.
- We propose an interference-aware PHY/FEC rate adaptation framework, InFRA, which selects the optimal PHY/FEC rates depending on the cause of packet losses.
- We propose a feedback protocol to support large scale video multicast, which requires minimal overhead while enabling fast adaptation.
- We implement InFRA with an open-source WLAN device driver, and our measurement results with off-the-shelf devices demonstrate that InFRA improves the performance significantly, especially when the interference is the major source of the packet losses.

The remainder of the paper is organized as follows: we discuss the related work in Section II, and address the impact of interference on multi-rate FEC-applied multicast in Sections III. We provide the detailed design of InFRA and evaluate the performance in Sections IV and V, respectively. Finally, we conclude the paper in Section VI.

II. Related Work

A. PHY/FEC Rate Adaptation for Multicast

Alay *et al.* [5] proposed to determine the optimal PHY/FEC rates that maximize the video bitrate. Based on the PLR fed back from the the receiver with the lowest PLR, AP determines whether to increase/decrease/keep its PHY rate. When the AP increases or decreases the PHY rate, it chooses the FEC rate as a predetermined value. If the AP keeps the current PHY rate, it chooses the FEC rate based on the current PLR value. With PLR estimation and an off-line PLR versus the optimal FEC rate table, X-Wing [7] determines the PHY rate achieving the maximum estimated throughput of the receiver with the lowest APLR. X-Wing assumes that PLR decreases by 5% as it decreases PHY rate by one step. Bulut *et al.* [8] proposed optimal PHY/FEC rate selection with IEEE 802.11n MIMO mode selection. According to the current 802.11 standard, however, multicast packets should be sent via legacy PHY rates, i.e., 802.11a PHY rates, and current off-the-shelf devices also utilize the legacy PHY rates for multicast.

None of the above approaches addresses the impact of interference on the multi-rate FEC-applied multicast, and hence, their PHY/FEC rate adaptation does not consider interference.

B. Wireless Video Transmission

Softcast [9] proposed a joint channel and source coding for scalable video streaming. The key idea of SoftCast is to enable the linear relationship between the pixel values and the transmitted signal by exploiting analog video coding and real-valued modulation. Parcast [10] enhanced Softcast with a design well-suited for MIMO-OFDM WLAN. These schemes require no feedback on wireless channel status, and the received video quality is automatically adjusted depending on the channel quality of each receiver. However, they require heavy modification to video codec and PHY layer. Futhermore, channel quality agnostic video transmission is vulnerable to interference, as high signal strength due to interference can be misinterpreted as a high pixel value.

C. Wireless Loss Differentiation

There are several studies on the differentiation of the cause of packet losses. CARA [4] and RRAA [11] differentiate the channel error and the collision by exploiting the request-to-send/clear-to-send (RTS/CTS) handshake. BLMon [12] and MiRA [13] diagnose the cause of losses by analyzing the aggregate MAC protocol data unit (A-MPDU) and block ACKs. However, such schemes are limited to the unicast service, since RTS/CTS, A-MPDU, and block ACK are not applicable to multicast. COLLIE [14] determines the cause of packet losses by analyzing symbol-level metrics, and REPE [15] detects the collision by sampling RSSI with a high frequency during the packet reception. However, both of them require heavy modification of the PHY layer. CDRA [16] detects collision based on RSSI and PLR, which can be applied to multicast. AP judges the existence of the interference with two fixed RSSI thresholds and a single PLR threshold. However, the criteria is too naive to work properly in a real environment, as the impact of interference is tightly coupled with the PHY rate.

III. Impact of Interference on Multi-rate FEC-applied Multicast

Interference from contending nodes or hidden nodes is a major source of packet losses in WLAN. In fact, various existing studies have shown that WLAN performance is highly affected by interference. A recent study [3] shows that interference causes burst packet losses intermittently in a large scale multicast network. Therefore, it is important to investigate the impact of the interference on PHY/FEC rate decision.

A. Measurement Setup

In order to investigate the impact of the interference on PHY/FEC rate decision, we conduct a simple experiment. Our measurement setup consists of four nodes: one AP, one STA, and two interferers (I1 and I2), equipped with Qualcomm Atheros AR9380 chipsets. The AP and the interferers are configured by Hostapd-2.5 [17]. In an auditorium with the layout shown in Fig. 1(a), we measure average APLR by varying the location of the STA and the interference type. The AP transmits FEC-encoded packets via multicast, where the employed FEC code is random linear network code (RLNC) [18] and the batch size (K) is fixed to 10. The determination of K will be discussed in Section IV-F. APLR is measured for three different combinations of (PHY rate, N): (i) initial setup (36 Mb/s, 12), (ii) PHY rate decrease (24 Mb/s, 12), and (iii) FEC rate decrease (36 Mb/s, 18). The

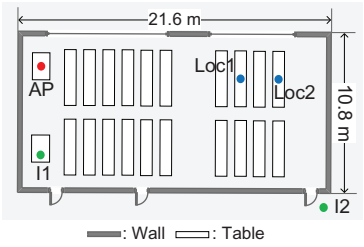

(a) Measurement topology.

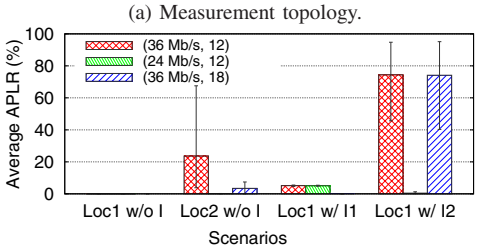

(b) Average packet loss rate.

Fig. 1. Preliminary measurement results.

two combinations, i.e., (24 Mb/s, 12) and (36 Mb/s, 18), incur similar airtime usages. The interferers broadcast the packets back-to-back using PHY rate of 6 Mb/s.

B. Measurement Results

Fig. 1(b) shows the average APLR for different scenarios. When the STA is located at Loc1 and all the interferers are disabled, all the three combinations work well. As the STA moves farther to Loc2, the initial setup, (36 Mb/s, 12), suffers from significant packet losses. Comparing the two possible options, i.e., decreasing PHY rate or FEC rate, we observe that decreasing PHY rate is more effective. On the other hand, when interference I1 is activated and the STA is at Loc1, decreasing PHY rate does not improve reliability. Since the packet losses are due to the nearby interferer, SINR becomes much lower than the required SINR for the decreased PHY rate, and hence, decreasing PHY rate increases the airtime only. On the other hand, decreasing the FEC rate increases the opportunities of accessing the channel without collision, thus reducing the packet losses.

For the last scenario, where the STA is at Loc1 and interference I2 is activated, the interferer and the AP are hidden from each other, and hence, APLR increases significantly with the initial setup. In this case, decreasing PHY rate reduces the packet losses significantly as the interfering signal strength is so low that decreasing PHY rate enables the STA to successfully receive packets even with the interference (i.e., the capture effect [19]). Whereas, decreasing FEC rate fails to decrease the APLR, since the burst losses due to hidden interference exceed the loss recovery capability of the FEC. From this measurement study, we verify that the effects of PHY and FEC rates are different from each other, and interference should be considered when determining PHY/FEC rates.

IV. InFRA: Interference-aware PHY/FEC Rate Adaptation Framework

A. Network Model and Objective

We consider an infrastructure mode WLAN that consists of an AP and multiple associated STAs. We assume low mobility of the STAs, e.g., the majority of users are seated and watching a common video. We consider real-time transport protocol/user datagram protocol (RTP/UDP)-based video streaming and the video packets are packetized as MPEG-2 TS (transport stream) format, which is a typical protocol for video multicast.

Our objective is to develop an interference-aware PHY/FEC rate adaptation framework for multi-rate FEC-applied multicast to minimize the airtime consumption while satisfying the following requirements.

- **Service level agreements (SLAs):** Given target APLR, S ($= 1\%$ [20]), and a node satisfaction ratio (NSR) threshold X (e.g., $X = 95\%$), InFRA aims at guaranteeing that at least X of the nodes experience APLR below S. The number of allowed unsatisfied nodes, U, is then determined by $U = \lfloor (1-X)Y \rfloor$, where Y is the number of total nodes. Since the user satisfaction is not linearly proportional to the APLR, e.g., typically the APLR below 1% is considered unacceptable for video streaming, the objective based on the target APLR is more practical.
- **Scalability:** Protocol overhead should be minimized to support a large number of receivers.
- **Fast recovery:** When SLA is not satisfied, immediate re-selection of PHY/FEC rates should be conducted.

B. Overall Architecture

We present an overview of InFRA architecture. Fig. 2 describes the overall architecture of InFRA, where the data flow and the internal information exchange are presented. We implement InFRA in the MAC-layer of both the AP and the STA with the modification of the off-the-shelf device driver. It is possible to implement InFRA of STA-side in a user space by using an application programming interface (API) to obtain the RSSI and CRC error notifications, as in Wireshark [21].

We adopt a request-based approach where each STA determines and reports the locally optimal PHY/FEC rates and AP chooses the network-wide PHY/FEC rates. This contrasts a centralized approach where the AP determines the optimal PHY/FEC rates based on the channel quality reports from STAs. Since interference relationship (interfering nodes and the signal strength) is heterogeneous for different receivers, we distribute the computation load to multiple receivers to support a large number of receivers.

In order to meet the APLR requirement, our design tries to find the PHY/FEC rates ensuring that the decoding failure ratio (DFR) is less than or equal to S (=1%).[3] Accordingly, each STA needs to receive at least 100 batches to measure the DFR of 1%, so it basically requests the PHY/FEC rates every 100 batches. Although such a long request period is less responsive, it is more stable since higher PHY/FEC rates are tried based on long-term statistics, which avoids frequent trials that might incur the packet losses. Moreover, it requires lower feedback overhead, which is beneficial for multicast.

[3]The rationale behind this is that 1) our framework should be transparent to the FEC codes including non-systematic codes where the APLR is the same as the DFR, and 2) it is more conservative in the case of the systematic codes in that the APLR requirement is satisfied if the DFR requirement is satisfied.

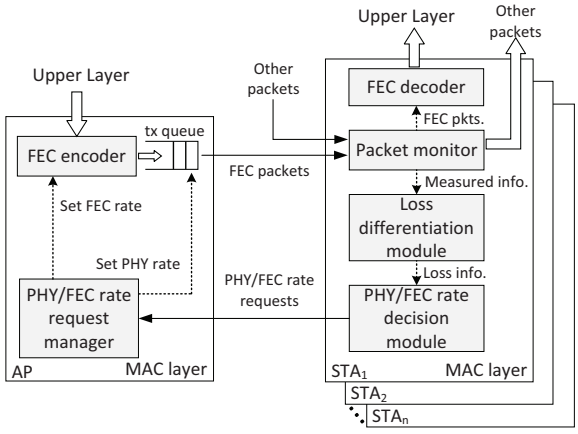

Fig. 2. Overview of InFRA architecture.

To support fast recovery, we make each STA send a request immediately when it fails to meet the target DFR, i.e., it fails to decode two batches out of the latest 100 batches.

1) AP-side Modules: The AP-side components are FEC encoder and PHY/FEC rate request manager. The FEC encoder generates N encoded packets per K packets. We control the FEC rate by controlling N, while fixing K. The PHY/FEC rate request manager collects the requests of PHY/FEC rates from STAs and determines whether the SLA is satisfied. It also determines the PHY/FEC rates to achieve the network-wide objective in Section IV-A, and the determined parameters are input to the FEC encoder and the transmit packet queue.

2) STA-side Modules: The STA-side components are FEC decoder, packet monitor, loss differentiation module, and PHY/FEC rate decision module. The FEC decoder gathers FEC-encoded packets and decodes them if possible. The decoded K original packets in a batch are then delivered to the upper layers. The packet monitor inspects the packet flow, and observes the existence of interfering nodes, and also measures the input values for the loss differentiation module that diagnoses the cause of measured packet losses. Specifically, it infers the portion of losses due to channel error and interference, which are used for determining PHY/FEC rates to request. The PHY/FEC rate decision module determines the best PHY/FEC rates and requests the determined parameters.

C. FEC Scheme

For FEC, we employ RLNC [18], which is a type of fountain codes (also called rateless codes). RLNC is simple yet erasure-resilient, and is widely used in many applications such as video streaming, cloud storage, and opportunistic routing [22]. We employ RLNC, but our design is transparent to the type of FEC codec, i.e., other FEC schemes such as Raptor [23] and Luby Transform (LT) codes [24] can also be used.

RLNC encodes a packet by taking a linear combination of K original packets with random coefficients. In the same way, RLNC can generate an arbitrary number of encoded packets.[4] Upon receiving K linearly independent packets, each receiver decodes and restores the original packets via matrix inversion.

In our scheme, each RLNC packet has a header including a batch ID, the generation size, a sequence number in the batch, and K encoding coefficients, and hence, each receiver can identify the packet loss using the sequence number.

D. STA-side Operation

1) Packet Monitor: The packet monitor measures the information used for loss differentiation by examining the incoming packets. The measured values are average RSSI from AP ($\overline{\gamma}_A$), current PHY rate of the batch (R_{cur}), current generation size of the batch (N_{cur}), the number of packet losses in the batch (L), the number of CRC errors (C), and the maximum RSSI of weak interference (γ_w), where the definition of weak interference is presented in the next subsection. Since FEC-encoded packets in a batch have the same length and are transmitted at the same PHY rate, we can infer whether a CRC-error packet is an FEC-encoded packet by examining the LENGTH and RATE elements in the SIGNAL field.[5] γ_w is the maximum RSSI value from the interfering nodes satisfying $\overline{\gamma}_A - \gamma_w \geq \delta(R_{min})$, where $\delta(R_{min})$ is the RSSI threshold for the minimum PHY rate. Whenever a packet with a new batch ID arrives, the packet monitor inputs the measured values to the loss differentiation module.

2) Loss Differentiation Module: The purpose of the loss differentiation module is to diagnose the cause of multicast packet losses in a standard-compliant manner. Since ACK, RTS/CTS, and A-MPDU based schemes are not applicable to multicast, InFRA utilizes RSSI and CRC error notifications, which are both available at WLAN receivers.

Loss Differentiation Metrics: RSSI is a per-packet measure of the received signal strength (RSS), and is available at every WLAN device. In most device drivers including ath9k, RSSI is a measure of signal power above the noise floor. Therefore, RSSI is equivalent to the SNR in the absence of interference, and hence, is proportional to the packet delivery ratio (PDR). However, PDR drops while RSSI increases when there is interference. When a packet with a low RSSI is lost, we can infer that it is due to channel error. In contrast, when a packet with a high RSSI is lost, we can infer that it is due to interference. Accordingly, RSSI can be used as a metric to determine the cause of packet losses, i.e., channel error or interference.

We conduct experiments to investigate the RSSI characteristics of FEC-encoded multicast packets. We apply the FEC with $K = 10$ and $N = 20$, and the coded packets are transmitted at different PHY rates (6 Mb/s to 54 Mb/s). We move along a predetermined path at a walking speed (about 0.5 m/s) and measure the standard deviation of RSSI in a batch and RSSI

[4]We employ a systematic approach that transmits K original packets and $N - K$ encoded packets rather than transmitting only N encoded packets. In addition to low complexity, a systematic code reduces APLR because it allows the received original packets to be salvaged when decoding fails.

[5]In order to provide the information for demodulation, the SIGNAL field in the PLCP (physical layer convergence procedure) header, transmitted at the minimum PHY rate, includes LENGTH and RATE elements indicating the length of the packet and the PHY rate used for the remaining part of the packet, respectively.

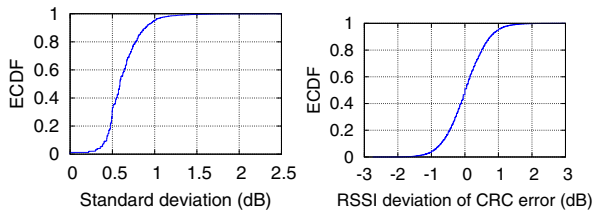

(a) (b)

Fig. 3. RSSI characteristics of the FEC-encoded multicast packets.

deviation of CRC-error packets, i.e., RSSI of CRC-error packet minus the average RSSI of the associated batch.

Fig. 3(a) shows the distribution of standard deviation of RSSI values in a batch. We observe that above 90% of batches show the standard deviation of under 1 (dB), and thus the RSSI variation in a batch is quite small. Fig. 3(b) shows the distribution of RSSI deviation of CRC-error packets, and most RSSI deviations are observed from -1 to 1. RSSI variation is low because the transmission time of a batch is smaller than the coherence time.[6] Therefore, we utilize the average RSSI of a batch as a metric to distinguish between the channel error loss and the interference loss. Another reason for adopting the average RSSI, not the individual RSSI, is that RSSI cannot be obtained for lost packets without CRC error notifications, e.g., due to preamble losses.

In Section III, we verified that decreasing PHY rate can be effective depending on the interfering signal strength. To this end, we define two types of interference: weak and strong interferences. Weak interference is defined as interference whose RSSI is smaller than the RSSI of the target packet by at least $\delta(R_{min})$ so that decreasing the PHY rate enables successful packet reception due to the capture effect. We define strong interference as interference whose RSSI is higher than the RSSI of the target packet minus $\delta(R_{min})$ so that decreasing the PHY rate does not enable the packet reception. When a packet is lost due to weak interference, the SIGNAL field transmitted at the minimum PHY rate is correctly received, but the CRC check fails. Then, if we decrease the PHY rate to the minimum PHY rate, packet losses due to weak interference can be prevented. Accordingly, we infer that a loss due to weak interference generates the CRC error notification, while a loss due to strong interference does not.

Our approach: We classify a total of L losses into l_{ch}, l_s and l_w, which denote the number of losses due to channel error, strong interference, and weak interference, respectively. Our algorithm examines the average RSSI ($\overline{\gamma}_A$), and if the average RSSI is smaller than the RSSI threshold of the current PHY rate, $\delta(R_{cur})$, all L losses are considered due to channel error.

The RSSI threshold is defined as the minimum RSSI required to ensure that PLR is lower than a target PLR, ρ (we choose $\rho = 0.1$ as in [26]), with a nominal packet length. Although a packet of a low RSSI might be lost due to interference, we regard it as the channel error since low RSSI implies the possibility of the channel error. In contrast, if the average RSSI is greater than or equal to the RSSI threshold, all L losses are inferred due to interference. As mentioned above, we determine that C and $(L-C)$ losses are considered due to weak interference and due to strong interference, respectively.

The differentiation process are expressed in (1).

$$(l_{ch}, l_s, l_w) = \begin{cases} (L, 0, 0), & \text{if } \overline{\gamma}_A < \delta(R_{cur}), \\ (0, L-C, C), & \text{otherwise.} \end{cases} \quad (1)$$

Fig. 4 presents the loss differentiation results of the STA in the measurement in Section III, with the initial setup, (36 Mb/s, 12). The number of losses are normalized by the number of total transmitted packets. When the STA is located at Loc2 without interference (Loc2 w/o I), our loss differentiation module regards the most losses as the channel error losses due to the low RSSI. When interference I1 is activated, which is closer to the AP (Loc1 w/ I1), the loss differentiation module then determines that the losses are due to the strong interference, since CRC error notifications are rarely observed. In the case of (Loc2 w/ I2), most losses incur the CRC error notifications, thus classified as the weak interference losses. Note that some packets are lost without CRC error notification when the preamble detection fails due to interference. Through this reult, we verify that the loss differentiation module diagnoses the cause of the packet losses appropriately.

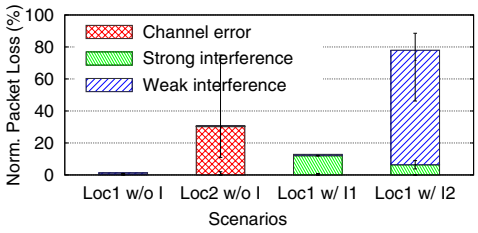

Fig. 4. Loss differentiation results in the measurement in Section III.

3) PHY/FEC Rate Decision Module: We define *RN pair* as a pair of PHY rate R and generation size N, which is denoted by $Q = (R, N)$ or Q for brevity. Each STA calculates the batch-level optimal *RN pair*, Q^{bat} for every batch, and based on that, each STA determines the *RN pair* to request, Q^{req}.

As discussed above, we consider two aspects to determine R: (i) RSSI from the AP and (ii) the capture effect when there is weak interference. To this end, we define two types of *RN pair*: (i) *RN pair* whose R is determined by the RSSI from AP, called channel-oriented *RN pair*, $\hat{Q} = (R_{ch}, N_{ch})$, where R_{ch} and N_{ch} are called channel-oriented R and N, and (ii) *RN pair* whose R is determined by the condition to induce the capture effect, called capture-inducing *RN pair*, $\tilde{Q} = (R_{cap}, N_{cap})$, where R_{cap} and N_{cap} are called capture-inducing R and N.

Determination of batch-level optimal Q: For a batch, each STA calculates two batch-level *RN pairs*, i.e., $\hat{Q}^{bat}$ and $\tilde{Q}^{bat}$. Algorithm 1 provides the formal description of the process. For the channel loss case (lines 1−8), i.e., if $\overline{\gamma}_A < \delta(R_{cur})$,

[6]The coherence time with 0.5 m/s at 5.8 GHz is about 43.5 ms according to Clarke's model [25], and the maximum batch transmission time with 6 Mb/s is 41.3 ms. In fact, as we limit the maximum N to 13 for 6 Mb/s as addressed later, the actual maximum batch transmission time in InFRA is smaller than 27 ms.

Algorithm 1 Determination of batch-level *RN pairs*

Input: $\overline{\gamma}_A, l_{ch}, l_s, l_w, R_{cur}, N_{cur}, \gamma_w$
Output: $\hat{Q}^{bat}$, $\tilde{Q}^{bat}$

1: **if** $\overline{\gamma}_A < \delta(R_{cur})$ **then** ▷ Channel loss
2: **if** $l_{ch}/N_{cur} > \rho$ **then**
3: $R_{ch} \leftarrow \text{GETRATE}(\overline{\gamma}_A)$, $l'_{ch} \leftarrow \lceil \rho N_{cur} \rceil$
4: **else**
5: $R_{ch} \leftarrow R_{cur}$, $l'_{ch} \leftarrow l_{ch}$
6: **end if**
7: $N_{ch} \leftarrow \left\lceil K \frac{N_{cur}}{N_{cur} - l'_{ch}} \right\rceil + \epsilon$
8: $\hat{Q}^{bat} \leftarrow (R_{ch}, N_{ch})$, $\tilde{Q}^{bat} \leftarrow \varnothing$
9: **else** ▷ Interference loss
10: **if** PRI condition is satisfied **then**
11: $R_{ch} \leftarrow R^{+}_{cur}$, $l'_{ch} \leftarrow \lceil \rho N_{cur} \rceil$
12: **else**
13: $R_{ch} \leftarrow R_{cur}$, $l'_{ch} \leftarrow 0$
14: **end if**
15: **if** $l_w == 0$ **then** ▷ Strong interference only
16: $N_{ch} \leftarrow \left\lceil K \frac{N_{cur}}{N_{cur} - l'_{ch} - l_s} \right\rceil + \epsilon$
17: $\hat{Q}^{bat} \leftarrow (R_{ch}, N_{ch})$, $\tilde{Q}^{bat} \leftarrow \varnothing$
18: **else** ▷ Weak interference
19: $N_{ch} \leftarrow \left\lceil K \frac{N_{cur}}{N_{cur} - l'_{ch} - l_s - l_w} \right\rceil + \epsilon$
20: $R_{cap} \leftarrow \text{GETRATE}(\overline{\gamma}_A - \gamma_w)$
21: $N_{cap} \leftarrow \left\lceil K \frac{N_{cur}}{N_{cur} - l_s} \right\rceil + \epsilon$
22: $\hat{Q}^{bat} \leftarrow (R_{ch}, N_{ch})$, $\tilde{Q}^{bat} \leftarrow (R_{cap}, N_{cap})$
23: **end if**
24: **end if**
25:
26: **function** GETRATE(γ)
27: Find out rate R s. t. $\delta(R) \leq \gamma < \delta(R^{+})$
28: **return** R
29: **end function**

only $\hat{Q}^{bat}$ is returned, since there is no weak interference loss. If the target PLR (ρ) is not satisfied by R_{cur} (line 2), R_{ch} is determined by the GETRATE function that finds the maximum R whose RSSI threshold is smaller than the input RSSI. As a result, we set the PHY rate ensuring that PLR is smaller than ρ by channel error. The estimated number of channel error losses for the new PHY rate, l'_{ch}, is then conservatively assumed to be $\lceil \rho N_{cur} \rceil$. Otherwise, R_{ch} and l'_{ch} remain to be the current values. N_{ch} is determined as the minimum N satisfying the following inequality:

$$N \cdot \frac{N_{cur} - l'_{ch}}{N_{cur}} \geq K. \tag{2}$$

We add a constant ϵ ($\epsilon = 1$) to handle unexpected losses.

For the interference loss case (lines 9−24), i.e., if $\overline{\gamma}_A \geq \delta(R_{cur})$, we increase the PHY rate when the RSSI is high enough to support a higher PHY rate. For a conservative design, we increase R_{ch} only to the next higher PHY rate than R_{cur} in the rate set, R^{+}_{cur}, as long as the conditions for PHY rate increase (PRI) are satisfied (line 10). In addition to the RSSI condition ($\overline{\gamma}_A \geq \delta(R^{+}_{cur})$), we adopt a history-based mechanism to avoid the failure due to impetuous PHY rate increase. When FEC decoding fails twice before receiving the latest 100 batches, InFRA records the failed PHY rate, R_{fail}, and limits the PHY rate under R_{fail} for a window (100 batches), which is doubled whenever it further fails to decode two batches before receiving 100 batches at R_{fail}.

If all losses are due to strong interference, N_{ch} are determined in a similar way to the channel loss case except for considering l_s (line 16), thus the algorithm returns $\hat{Q}^{bat}$ only. On the other hand, if some portion of the losses are due to weak interference, the algorithm returns another *RN pair*, $\tilde{Q}^{bat} = (R_{cap}, N_{cap})$, as well as $\hat{Q}^{bat}$. R_{cap} is determined by the RSSI difference between the maximum weak interference (γ_w) to induce the capture effect. Note that the increase of RSSI due to weak interference is marginal since the signal strength of the weak interference is much smaller than RSSI from the AP (smaller by at least 8 dB). Therefore, the RSSI difference is assumed to be the same as the signal-to-interference ratio (SIR). Although there is a report that SIR threshold is lower than the SNR threshold [27], we use the same threshold values for the channel error case (line 3) for the sake of simple and conservative operations.

We assume that weak interference losses will be removed with R_{cap}, as R_{cap} is determined by considering the maximum weak interference. Since R_{cap} is inherently lower than R_{ch}, the expected number of channel errors is assumed to be zero. We then determine N_{cap} by considering l_s only (line 21).

Update of R and N: We find $\hat{Q}^{req}$ and $\tilde{Q}^{req}$ satisfying at least 99 batches out of the latest 100 batches. For this purpose, in addition to keeping track of the most conservative parameters (minimum R and maximum N) from Q^{bat}'s, we also update the second minimum R and the second maximum N. We take the second minimum and maximum values into account to avoid over-provisioning due to the most conservative parameters, since the determination of Q^{bat} is based on conservative estimation of channel error and adoption of ϵ.

The minimum and the second minimum R's (R^{min}_{ch}, R^{2ndmin}_{ch}, R^{min}_{cap}, and R^{2ndmin}_{cap}) and the maximum and the second maximum N's (N^{max}_{ch}, N^{2ndmax}_{ch}, N^{max}_{cap}, and N^{2ndmax}_{cap}) are updated for every batch. When more than one batch return the same maximum N, the second maximum N is set to the maximum value. The same rule is applied to R.

PHY/FEC rate request: Depending on the type of the request, i.e., a regular or an event-driven request, $\hat{Q}^{req}$ and $\tilde{Q}^{req}$ are determined in different ways. For $\hat{Q}^{req}$, in the case of the regular request, we compare the required airtime of the following two Q's: $(R^{min}_{ch}, N^{2ndmax}_{ch})$ and $(R^{2ndmin}_{ch}, N^{max}_{ch})$. Note that both Q's guarantee the DFR requirement that allows decoding failure of the maximum one batch out of the latest 100 batches, as decoding of all the batches are expected to be successful except for the single batch that could be satisfied by $(R^{min}_{ch}, N^{max}_{ch})$.

Among the two candidates, Q requiring less airtime is chosen. Similarly, we determine $\tilde{Q}^{req}$ requiring less airtime among $(R^{min}_{cap}, N^{2ndmax}_{cap})$ and $(R^{2ndmin}_{cap}, N^{max}_{cap})$. When a STA sends an event-driven request, the STA requests the most conservative parameters: $\hat{Q}^{req} = (R^{min}_{ch}, N^{max}_{ch})$ and $\tilde{Q}^{req} = (R^{min}_{cap}, N^{max}_{cap})$. The PHY/FEC rate request messages are sent via unicast. In order to alleviate the congestion and contention, each STA defers a random interval from 0 to T_r before the request.

TABLE I
DEFAULT RSSI THRESHOLD AND MAXIMUM GENERATION SIZE.

R (Mb/s)	6	12	18	24	36	48	54
$\delta(R)$ (dB)	8	11	14	17	20	23	26
N_{max}	13	24	34	42	55	65	69

E. AP-side Operation

Based on the PHY/FEC requests from STAs, AP finds the network-wide *RN pair*, $Q^{net} = (R^{net}, N^{net})$ satisfying at least X (=95%) of the receivers (at least $Y - U$ receivers). AP re-selects Q^{net} upon receiving event-driven requests from more than U receivers or after sending the latest 100 batches and waiting additional T_r. Q requiring the least airtime is selected among four candidates: $(R_{ch,Y-U}, N_{ch,1})$, $(R_{ch,Y}, N_{ch,U+1})$, $(R_{cap,Y-U}, N_{cap,1})$, and $(R_{cap,Y}, N_{cap,U+1})$, where the second subscription value means the descending order in each parameter, e.g., if $Y = 20$ and $U = 1$, $R_{ch,Y-U}$ means the 19th largest (2nd-minimum) value in R_{ch}'s and $N_{cap,U+1}$ means the 2nd maximum value in N_{cap}'s. For the same reason as in the previous subsection, all the four candidate Q's satisfy the NSR requirement.

We limit N^{net} to a maximum generation size, N_{max}, dependent on R^{net}, considering the delay and the bandwidth as detailed below.

F. Practical Issues

1) RSSI Threshold Calibration: It is known that the RSSI-PDR relationship differs depending on the devices [28]. To overcome this, we develop an on-line calibration of the RSSI thresholds on top of the default RSSI thresholds obtained from our off-line measurements (Table I). Note that we skip the 9 Mb/s due to its inferior performance to 12 Mb/s as in the IEEE 802.11n standard [29]. Whenever receiving the measured results from the packet monitor, the calibration module records the number of received packets and lost packets according to the measured average RSSI. The measured RSSI values are indexed relatively to the current RSSI threshold for a given PHY rate. When the sample is gathered sufficiently, the calibration module updates the RSSI threshold based on the measurement. To remove the effect of interference, the data are recorded only when interference is not detected.

2) FEC Parameters (K and N_{max}): We determine K and N_{max} by considering the delay and the bandwidth, while existing schemes determine them arbitrarily, e.g., $K = 100$ and $N_{max} = 300$ in [7]. Such a large K value incurs a large buffering delay at the FEC encoder, as the encoder waits for K packets to arrive. Whereas, N_{max}/K is related to the throughput and should be limited by the wireless bandwidth. Assuming the range of video bitrates in consideration is from 1 to 3 Mb/s, we choose K as 10, which requires maximum buffering delay of about 100 ms, and N_{max} for each PHY rate as in Table I, requiring 80% of the total wireless bandwidth.

V. PERFORMANCE EVALUATION

We comparatively evaluate the performance of InFRA under various scenarios. We have implemented InFRA by modifying the latest ath9k device driver, backport 4.2.6-1.

TABLE II
NOTATION AND PARAMETER VALUES USED IN EXPERIMENTS.

Symbol	Definition	Exp. Val.
K	Batch size	10
S	Target APLR	1%
X	Target node satisfaction ratio	95%
Y	Number of total receivers	20
U	Number of allowed unsatisfied receivers	1
T_r	Maximum request deferring time	200 ms

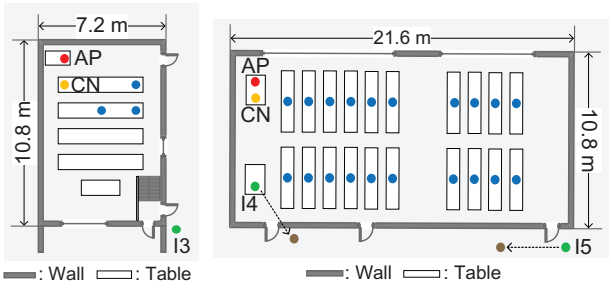

(a) Classroom (b) Auditorium

Fig. 5. Measurement topology.

A. Measurement Setup

We conduct our experiments in two different places: (1) a classroom and (2) an auditorium, where both the floor plans are shown in Fig. 5. The AP and multiple STAs (3 and 20 for the small and large-scale experiments, respectively) constitute a WLAN using a channel in 5 GHz band, not occupied by other pre-deployed APs. HP-ProBook-450-G2 with AR9380 chipset is configured as the AP by using Hostapd, and the same type of laptops are used for STAs, where 17 and 3 STAs are equipped with AR9380 and AR9462, respectively. Ubuntu 14.04 is installed in the laptops. A STA is configured as a capturing node (CN) with the monitor mode to measure the airtime. We use the parameter values listed in Table II, and the following performance metrics are measured: (i) *APLR*, (ii) *NSR*, i.e., the fraction of nodes that satisfy target APLR, (iii) *Fractional airtime*, i.e., the fraction of airtime occupancy by multicast sessions, and (iv) *Peak signal to noise ratio (PSNR)*, a widely-adopted video quality metric [30].

We compare InFRA with the following schemes:
(1) *Fixed PHY/FEC rates:* various combinations of R and N. We evaluate the fixed schemes for all possible combinations of R (= 6, 12, 18, 24, 36, 48, and 54 Mb/s) and N (= 13, 15, 20, and 25).
(2) *X-Wing* [7]: a modified version for fair comparison. The original X-Wing employs the bounded LT code with $K = 100$ and $N_{max} = 300$, and the target APLR S is set to 10%. In order to eliminate the effect from the difference of the FEC schemes and the target values, we employ the RLNC with $K = 10$ and $N_{max} = 30$, and set S to 1%.

B. Small Scale Evaluation

In order to investigate the detailed operation of InFRA, we conduct small-scale experiments where three STAs are associated with an AP and a hidden interferer (I3) exists, as presented in Fig. 5(a). We generate constant bit rate (CBR) traffic of 2 Mb/s from the AP to STAs using Iperf 2.0.5 with fixed packet length of 1,328 bytes according to the

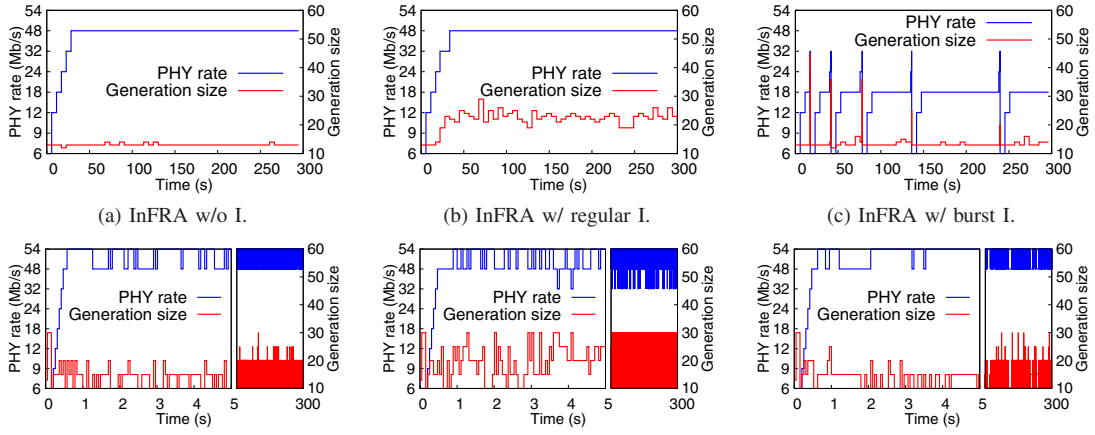

(a) InFRA w/o I. (b) InFRA w/ regular I. (c) InFRA w/ burst I.

(d) X-Wing w/o I. (e) X-Wing w/ regular I. (f) X-Wing w/ burst I.

Fig. 6. Transition of PHY rate and generation size under different scenarios.

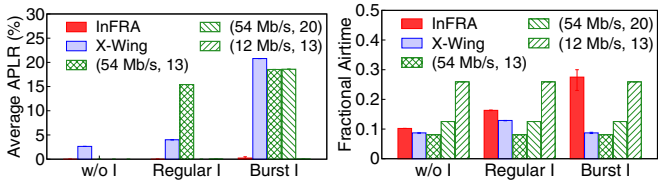

(a) Average APLR. (b) Fractional airtime.

Fig. 7. Average APLR and fractional airtime for each small-scale scenario.

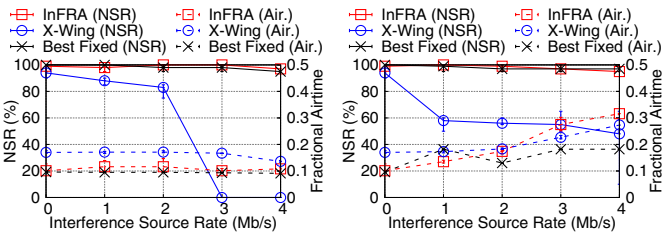

(a) w/ I4. (b) w/ I5.

Fig. 8. NSR and fractional airtime w.r.t. source rate of interference.

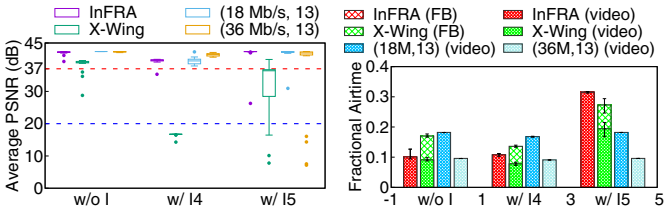

(a) Average PSNR. (b) Fractional airtime.

Fig. 9. Average PSNR and fractional airtime for each large-scale scenario. The box plot describes the median (line within the box), inter-quartile range (upper and lower borders of the box), maximum and minimum values within in 1.5 inter-quartile range (whiskers), and the outliers (circles).

standard MPEG-2 TS with RTP packet format. We evaluate the performance of InFRA and X-Wing under three different scenarios: (i) no interference, (ii) regular interference (CBR of 1.5 Mb/s), and (iii) burst interference (periodic on-off pattern whose on and off durations are 0.5 s and 2.5 s, respectively). The MPDU size and the PHY rate of the interferer are set to 1,400 bytes and 6 Mb/s, respectively.

Fig. 6 presents the snapshots on how InFRA and X-Wing select the PHY rate and the generation size, (R, N), under different scenarios. When there is no interference (Figs. 6(a) and 6(d)), InFRA chooses 48 Mb/s continuously since it determines R based on long-term statistics while keeping N small enough to handle intermittent losses. X-Wing oscillates between 48 and 54 Mb/s, thus losing some packets. X-Wing sets N to 10 whenever all the receivers decode a batch, but such an aggressive protection cannot prevent packet losses in advance. When regular interference is generated (Figs. 6(b) and 6(e)), both InFRA and X-Wing increase N as it is more efficient than decreasing R. In the burst interference case (Figs. 6(c) and 6(f)), when the burst losses exceed the loss recovery capability of FEC, InFRA decreases R while X-Wing keeps losing packets as it has no mechanism to handle burst losses due to interference. We observe that InFRA increases the interval between the trials to the higher PHY rate by the history-based mechanism.

Fig. 7 presents the average APLR and the fractional airtime. We compare the performance with the three fixed parameters: (54 Mb/s, 13), (54 Mb/s, 20), and (12 Mb/s, 13), the best fixed parameters for scenarios 1, 2, and 3, respectively. In Fig. 7(a), we observe that many packets are lost due to burst interference except for InFRA and (12 Mb/s, 13). Note that different nodes experience a similar level of losses. As shown in Fig. 7, the best fixed parameter varies depending on the scenarios, and InFRA meets the APLR requirement and consumes slightly longer airtime than the best fixed parameters under all the scenarios. On the other hand, X-Wing fails to meet the APLR requirement for the aforementioned reasons.

C. Large Scale Evaluation

We evaluate the performance with 20 STAs in the auditorium shown in Fig. 5(b). With streaming a real video clip (1280x720 resolution, MPEG-4 codec, 2 Mb/s, 5 min), we measure the performance for the various source rates of the interference. The other settings of the interference are the same as in Section V-B.

Fig. 8 presents the NSR and the fractional airtime with respect to the interference source rates. InFRA achieves the target NSR (=95%) while requiring a similar airtime to the best fixed parameters. In the case of X-Wing, NSR decreases as the interference source rate increases, and some nodes

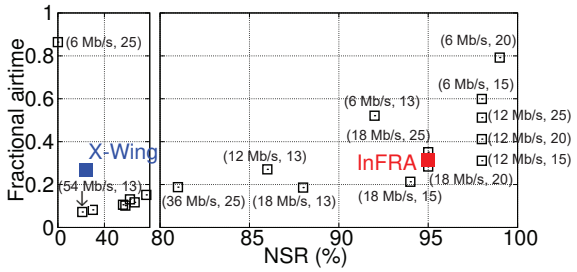

Fig. 10. NSR and fractional airtime under interference with YouTube traffic.

with good channel quality receive the packets with the hidden interference, thus yielding larger NSRs than those with the contention interference. In average, InFRA achieves 2.3x and 1.8x higher NSR than X-Wing with interference I4 and I5, respectively. With the contending node, the amount of packet loss is smaller than that with the hidden node, and hence, the required airtime is less than the hidden interference case.

Fig. 9 presents the PSNR values across the receivers and the breakdown of the fractional airtime under the selected three scenarios: (i) no interference, (ii) contention interference (CBR of 4 Mb/s), and (iii) hidden interference (CBR of 4 Mb/s). Besides X-Wing, we compare InFRA with the selected fixed parameters, (36Mb/s, 13) and (18Mb/s, 13), which are the best for scenarios 1 and 2, and scenario 3, respectively.

In Fig. 9(a), PSNR values of 20, 25, 31, and 37 are mapped to mean opinion score (MOS) of 2 (poor), 3, 4, and 5 (excellent), respectively [30]. InFRA provides the excellent-quality of video to at least 19 receivers, while some receivers are poorly served with X-Wing. In Fig. 9(b), we present the portion of feedback (FB) packets. InFRA requires to send the feedback (PHY/FEC rate request) once every 100 batches, while X-Wing sends three feedback packets every batch. Accordingly, X-Wing incurs much larger feedback overhead than InFRA. In the case of X-Wing with interference I4, the feedback overhead decreases as some feedback packets collide with the interference packets. Note that in scenario 3, InFRA requires large airtime since it chooses a low PHY rate due to the conservative selection of PHY rate in the weak interference case. Designing more efficient PHY rate selection with the weak interference is our future work.

We finally evaluate the performance when the interference traffic is real YouTube traffic. Both interference I4 and I5 are activated, where each interferer streams a YouTube video (1280x720p resolution and 1.2 Mb/s [31]) to a closely located STA, as shown in Fig. 5(b). Fig. 10 presents the NSR and the fractional airtime of InFRA and all the comparison schemes. In this figure, the performance improves as the point goes toward the bottom right direction. We observe that InFRA achieves the performance similar to the best fixed PHY/FEC scheme under the real environment.

VI. Conclusion

We proposed InFRA to differentiate the selection of PHY/FEC rates along with th cause of packet losses based on RSSI and CRC error notifications. The elaborate framework of the PHY/FEC rate decision enables efficient and interference-resilient multicast service with minimal overhead. From extensive evaluation with prototype implementation, we demonstrate that InFRA enhances the multicast delivery, achieving 2.3x and 1.8x higher NSR with a contention interferer and a hidden interferer, respectively, compared with the state-of-the-art PHY/FEC rate adaptation scheme.

VII. Acknowledgements

This work was supported by the National Research Foundation of Korea (NRF) grant funded by Korea government (MSIP) (NRF-2015R1A2A2A01006750).

References

[1] Cisco Visual Networking Index, "Global Mobile Data Traffic Forecast Update, 2015–2020," *White paper*, 2015.
[2] IEEE 802.11aa, *Part 11: Wireless LAN Medium Access Control (MAC) and Physical Layer (PHY) Specifications Amendment 2: MAC Enhancements for Robust Audio Video Streaming*, IEEE Std., 2012.
[3] V. Gupta *et al.*, "Experimental Evaluation of Large Scale WiFi Multicast Rate Control," in *Proc. IEEE INFOCOM*, 2016.
[4] J. Kim *et al.*, "CARA: Collision-Aware Rate Adaptation for IEEE 802.11 WLANs," in *Proc. IEEE INFOCOM*, 2006.
[5] Ö. Alay *et al.*, "Dynamic Rate and FEC Adaptation for Video Multicast in Multi-rate Wireless Networks," *Mobile Netw. Appl.*, vol. 15, no. 3, pp. 425–434, 2010.
[6] J. Xiong and R. R. Choudhury, "Peercast: Improving link layer multicast through cooperative relaying," in *Proc. IEEE INFOCOM 2011*, 2011.
[7] S. H. Wong *et al.*, "X-WING: A High-Speed Wireless Broadcasting Framework for IEEE 802.11 Networks," in *Proc. IEEE SECON*, 2013.
[8] B. Bulut *et al.*, "Cross-layer Design of Raptor Codes for Video Multicast over 802.11n MIMO Channels," in *Proc. IEEE PIMRC*, 2015.
[9] S. Jakubczak and D. Katabi, "A Cross-layer Design for Scalable Mobile Video," in *Proc. ACM MobiCom*, 2011.
[10] X. L. Liu *et al.*, "Parcast: Soft Video Delivery in MIMO-OFDM WLANs," in *Proc. ACM MobiCom*, 2012.
[11] S. H. Wong *et al.*, "Robust Rate Adaptation for 802.11 Wireless Networks," in *Proc. ACM Mobicom*, 2006.
[12] R. Anwar *et al.*, "Loss Differentiation: Moving onto High-speed Wireless LANs," in *Proc. IEEE INFOCOM*, 2014.
[13] I. Pefkianakis *et al.*, "MIMO Rate Adaptation in 802.11n Wireless Networks," in *Proc. ACM Mobicom*, 2010.
[14] S. Rayanchu *et al.*, "Diagnosing Wireless Packet Losses in 802.11: Separating Collision From Weak Signal," in *Proc. IEEE INFOCOM*, 2008.
[15] J.-H. Hauer *et al.*, "Mitigating the Effects of RF Interference Through RSSI-based Error Recovery," in *Proc. European Conference on Wireless Sensor Networks*, 2010.
[16] C. Zhou *et al.*, "Collision-Detection Based Rate-Adaptation for Video Multicasting over IEEE 802.11 Wireless Networks," in *Proc. IEEE ICIP*, 2010.
[17] HostApd: IEEE 802.11 AP, IEEE 802.1X/WPA/WPA2/EAP/ RADIUS Authenticator. https://w1.fi/hostapd/.
[18] T. Ho *et al.*, "A Random Linear Network Coding Approach to Multicast," *IEEE Trans. Inf. Theory*, vol. 52, no. 10, pp. 4413–4430, 2006.
[19] J. Lee *et al.*, "An Experimental Study on The Capture Effect In 802.11a Networks," in *Proc. ACM WiNTECH*, 2007.
[20] J. Prado *et al.*, "Application Characteristics for HT Usage Scenarios," IEEE 802.11-03/364r0, 2003.
[21] Wireshark 2.2.3. [Online]. Available: https://www.wireshark.org/
[22] M. Médard *et al.*, "Network Coding Mythbusting: Why It Is Not About Butterflies Anymore," *IEEE Communications Magazine*, vol. 52, no. 7, pp. 177–183, 2014.
[23] A. Shokrollahi, "Raptor Codes," *IEEE Trans. Inf. Theory*, vol. 52, no. 6, pp. 2551–2567, 2006.
[24] M. Luby, "LT-codes," in *Proc. 43rd Annu. IEEE Symp. Foundations of Computer Science (FOCS)*, 2002.
[25] T. S. Rappaport *et al.*, *Wireless Communications: Principles and Practice*. Prentice Hall PTR New Jersey, 1996, vol. 2.
[26] J. Zhang *et al.*, "A Practical SNR-guided Rate Adaptation," in *Proc. IEEE INFOCOM*, 2008.
[27] D. Son *et al.*, "Experimental Study of Concurrent Transmission in Wireless Sensor Networks," in *Proc. ACM SenSys*, 2006.
[28] G. Judd *et al.*, "Efficient Channel-aware Rate Adaptation in Dynamic Environments," in *Proc. ACM MobiSys*, 2008.
[29] *Wireless LAN Medium Access Control (MAC) and Physical Layer (PHY) Specifications*, IEEE Std. 802.11-2016 (Revision of IEEE Std. 802.11-2012), 2016.
[30] J. Klaue *et al.*, "Evalvid–A framework for video transmission and quality evaluation," in *Proc. 13th Int. Conf. TOOLS*, 2003.
[31] YouTube. [Online]. Available: https://www.youtube.com/watch?v=ttz4Sr0tZFg/